Polym. Bull. (2012) 69:795–806
DOI 10.1007/s00289-012-0773-3

ORIGINAL PAPER

Synthesis and encapsulation of magnetite nanoparticles in PLGA: effect of amount of PLGA on characteristics of encapsulated nanoparticles

Kittima Bootdee · Manit Nithitanakul · Brian P. Grady

Received: 13 October 2011 / Revised: 18 March 2012 / Accepted: 21 May 2012 /
Published online: 21 June 2012

Abstract Oleic acid-coated superparamagnetic iron oxide nanoparticles (Fe_3O_4) encapsulated within poly(D,L-lactide-*co*-glycolide) (PLGA) particles were prepared by the w/o/w emulsion technique using poly(vinyl alcohol) as a dispersant. The concentration of PLGA in the oil phase was varied (5, 15, 30, 45, and 60 mg/ml) at constant magnetite concentration in the oil phase (5 mg/ml) to study the properties of composite Fe_3O_4–PLGA nanoparticles. Even though PLGA concentration varied widely in the oil phase, the weight percent of 7–16 nm diameter magnetite in the particles varied only from 56 to 62 % (23–28 vol.%). The obtained composite nanoparticles were essentially spherical with magnetite spatially uniformly dispersed in individual PLGA particles, as measured by transmission electron microscopy (TEM). Also, the magnetite concentration in each particle did not vary widely as determined qualitatively via microscopy. Hydrodynamic diameters of the composite nanoparticles as measured by dynamic light scattering increased by approximately 10 % with added magnetite, with a smaller relative increase in diameter measured by TEM. The zeta potential of the particles was about −26 mV, independent of Fe_3O_4 loading. Relatively high saturation magnetizations (36–45 emu/g) were measured for these highly loaded particles, with the latter value only 7 emu/g lower than the value measured for the oleic acid-coated particles alone.

Keywords Nanoparticles · Magnetite · Superparamagnetic iron oxide · Double-emulsion method

K. Bootdee · M. Nithitanakul (✉)
The Petroleum and Petrochemical College, Chulalongkorn University, Bangkok, Thailand
e-mail: manit.n@chula.ac.th

B. P. Grady
University of Oklahoma School of Chemical, Biological and Materials Engineering, Norman, OK, USA

Introduction

Magnetic nanoparticles (MNP) have been investigated for various biomedical applications, such as biomagnetic separation, tumor hyperthermia, retial detachment therapy, improve MRI diagnostic contrast agent, and magnetic field guided for carrier drug or radioactive therapies localized to specific cell [1, 2]. The application of drug delivery is of particular interest for these particles. Use of an external magnetic field with magnetic nanoparticles could effectively carry drugs directly to specific tissue in the body [3]. Superparamagnetic iron oxide nanoparticles (Fe_3O_4) have ability to enhance magnetic resonance contrast and improve delivery systems. Pre-clinical studies indicate that some shortcomings of magnetic drug carriers, such as toxicity [4], poor penetration depth, and diffusion of the released drug from the disease site [5], can be overcome by improvement in magnetic targeted carriers design. Furthermore, encapsulating Fe_3O_4 in another particle for controlled release of a drug is an area of intense interest.

Magnetic nanoparticles distributed in a matrix of biodegradable polymer have also been reported to be released in a controlled fashion with respect to both time and location [6]. Encapsulated Fe_3O_4 within a biocompatible polymer can form stable non-toxic aqueous dispersions. Encapsulating Fe_3O_4 has resulted in reduced aggregation and lower toxicity [7]. The most common polymers are hydrophobic polyesters such as poly(D,L-lactide-*co*-glycolide) (PLGA), poly(D,L-lactide) (PLA), and poly(glycolide) (PGA) [8].

PLGA copolymers are significant for tissue engineering applications and delivery system because they are biodegradable, biocompatible, non-toxic [9], and approved by the U.S. Food and Drug Administration for use inside the body [10]. Spheres with sub-micron and micron diameters are able to release drug over long periods of time. For example, PLGA microparticles encapsulating a decoy oligodeoxynncleotide (ODN) against nuclear facto-κB (NF-κB) able to release decoy ODN at a constant rate for about 40 days [11]. Blanco-Príeto et al. [12] studied the drug release behavior of gentamicin (GM) loaded in PLGA microsphere and found that GM released continuously up to 4 weeks after an initial burst release. PLGA microparticles with higher loading release GM faster. Microsphere size has a significant effect on the efficient of drug loading and drug release rate and can potentially be varied to design a drug delivery system controlled with desired release profile. Mathematical modeling provides prediction of the effect of mean diameter on drug release [13]. Piroxicam-loaded PLGA microsphere having mean size from 13.5 to 76 μm showed a reduction in the initial release rate with an increase in microsphere size [13].

Several methods have been developed to prepare magnetic nanoparticles encapsulated in small polymeric particles including water-in-oil (w/o) single emulsion, water-in-oil-in-water (w/o/w) double emulsion, coacervation [14], inverse microemulsion-, and miniemulsion-polymerization [15]. The criteria used to evaluate a particular method is encapsulation efficiency (a measure of the number of magnetic particles in the reaction mixture that are encapsulated), dispersion of the magnetic particles in the polymer particles (magnetization is a good measure since agglomeration tends to reduce magnetization, and transmission electron microscopy

can also be used for a more direct measurement) and distribution of magnetic particles among all polymer particles (all particles should contain approximately the same number of magnetic particles). The encapsulation methods listed above are all suitable for oil-soluble drugs, while w/o/w double emulsion is best suited to encapsulate water-soluble drug including vaccines, proteins, and peptides [14].

In this study, Fe_3O_4 was encapsulated within PLGA microparticles by using an emulsification-diffusion technique. A w/o/w emulsion was used with the Fe_3O_4 and the polymer in the oil phase [6]. The purpose of these experiments was to determine the effect of PLGA concentration in the oil phase at constant magnetite concentration on the particle characteristics including encapsulation amount, particle size, surface charge, and magnetization behavior. Our goal was to produce particles with high magnetizations, since the higher the magnetization, the higher the magnetic force produced for a given magnetic field.

Materials and methods

Materials

PLGA (50:50 lactide/glycolide, M_w 40–75 kDa) was purchased from Sigma Chemical Co. (St. Louis, MO, USA). Polyvinyl alcohol (PVA) (M_w 30–70 kDa), ferrous chloride tetrahydrate (99 %), ferric chloride hexahydrate (99 %), and oleic acid (90 %) were purchased from Sigma-Aldrich Chemical Co. (St. Louis, MO, USA). Chloroform was purchased from ACI Labscan (Thailand). Ammonium hydroxide (25 wt% NH_3 in water) was purchased from Suksapanpanich Co (Thailand). All reagents were used as received.

Synthesis of hydrophobic magnetite

Preparation of oleic acid-coated on magnetite nanoparticles was carried out using procedure described by Hamoudeh [16]. 24.3 g of $FeCl_3{\cdot}6H_2O$ and 12 g of $FeCl_2{\cdot}4H_2O$ were dissolved in 50 ml of deionized water under nitrogen gas. Forty millilitre of NH_4OH (25 %) was then added at 70–80 °C. Oleic acid (OA) (40 %, w/w of calculated magnetite amount) was added dropwise during 10 min and heated for 30 min. The black lump-like gel was separated by magnetic decantation and cooled to room temperature and then washed several times with deionized water and acetone to remove excess OA.

Preparation of PLGA nanoparticles

Nanosphere-containing Fe_3O_4 were prepared by double-emulsion technique as described by Wassel [6]. Five milligram per millilitre of magnetic nanoparticles was dispersed into 1 ml of chloroform. PLGA (5, 15, 30, 45, and 60 mg/ml) was then dissolved in the solution, and 200 µl of deionized water were emulsified in the PLGA/Fe_3O_4/chloroform solution by sonification on ice for 1 min to form a water-in-oil emulsion. For the largest concentration, 60 mg/ml, not all of the PLGA

dissolved; however, the undissolved material was believed to have been separated during subsequent processing steps since no evidence was found in TEM micrographs of this undissolved material. This first emulsion was emulsified again by adding 6 ml of deionized water-containing 2 % PVA. The resulting w/o/w emulsion was sonicated on ice again for 5 min (used 56 % amplitude for sonicated at the first oil phase and 96 % amplitude at the second emulsion with probe size was 1½ inch and 3 inch for vessel size in diameter) and stirred for ~24 h to allow solvent evaporation and nanoparticles formation. PLGA nanoparticles were isolated by centrifugation at 15,000 rpm for 30 min at 4 °C, washed four times with deionized water to remove any access PVA and Fe_3O_4, and were dispersed in 1 ml of deionised water in 2 ml cryotubes. The PLGA nanoparticles were then lyophilized for 2 days and stored in a desiccator prior to use. Pure PLGA nanoparticles, e.g., no magnetite was added, at a PLGA concentration of 5 mg/ml to compare to those made with magnetite.

Characterization of OA-coated magnetic nanoparticles

Fourier transform infrared spectra (FTIR)

FTIR spectra of the magnetite nanoparticles were collected on a FTIR spectrometer (Thermo Nicolet, Nexus 670). The powder samples were ground with KBr and compressed into a pellet whose spectra were record. A drop of neat OA was placed on a ZnSe plate, and the spectrum was recorded and used as a reference.

Transmission electron microscopy (TEM)

Particle morphology, size, and structure of OA-coated Fe_3O_4 were determined by TEM (H-7650 Hitachi transmission electron microscope). The aqueous dispersion was drop-case onto formvar-copper grid. The sample was dried prior to placing in the TEM for analysis.

Characteristic of PLGA/Fe_3O_4 nanoparticles

Dynamic light scattering and zeta potential

A Malvern Zetasizer Nano Series was used for dynamic light scattering to determine hydrodynamic particle size as well as zeta potential. Measurements were performed at 25 °C. Viscosity and refraction index of the continuous phase were set to values appropriate for water.

Transmission electron microscopy

Particle size and the qualitative state of aggregation of the Fe_3O_4 inside PLGA nanoparticles were determined by TEM (H-7650 Hitachi transmission electron microscope). Composite particles were dropped onto formvar-coated copper grid and placed in the TEM for analysis.

Magnetization measurement

Magnetization of encapsulated Fe_3O_4 was measured by vibrating sample magnetometer (VSM, LakeShore 7404) at room temperature.

Thermogravimetric analysis (TGA)

Magnetite loading in the PLGA nanoparticles was determined by a thermogravimetric analyzer (TGA, DuPont, model TGA 2950). Samples were placed in an aluminum pan and subsequently heated from 30 to 800 °C at a rate of 20 °C/min in air.

Results and discussion

Hydrophobic magnetite

OA-coated magnetite nanoparticles were analyzed by TEM (see Fig. 1). Agglomerates of individual particles were observed which almost certainly occurred during TEM sample preparation [17]. Particle diameters ranged from 7 to 16 nm with an average diameter 10.6 ± 2.3 nm which is similar to the sizes reported in previous study (5–15 [6], ~12 [16], and 9 nm [18]).

FTIR spectroscopy was used to study adsorption of OA on the surface of Fe_3O_4. Figure 2 shows the typical FTIR spectra of pure OA (Fig. 2a), and iron oxide nanoparticles coated with OA (Fig. 2b). For pure OA, the two bands at 2,925 and 2,855 cm^{-1} were attributed to the asymmetric CH_2 stretch and the symmetric CH_2 stretch, respectively. The peak at 1,713 cm^{-1} is attributed to the C=O stretch, and the band at 1,285 cm^{-1} was a result of the C–O stretch. Bands appearing at 1,465 and 936 cm^{-1} indicate O–H in-plane and out-of-plane stretching, respectively. In

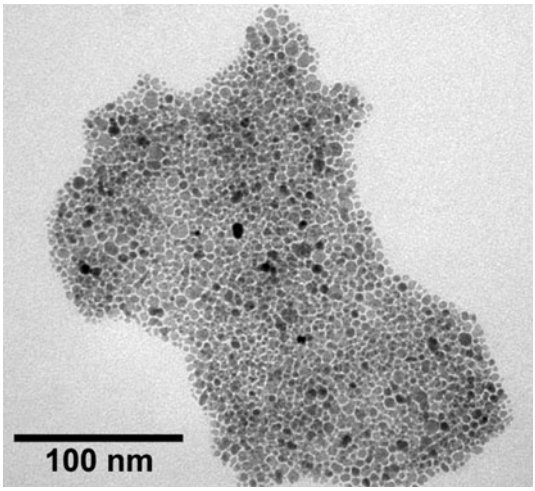

Fig. 1 TEM image of OA-coated magnetite nanoparticles

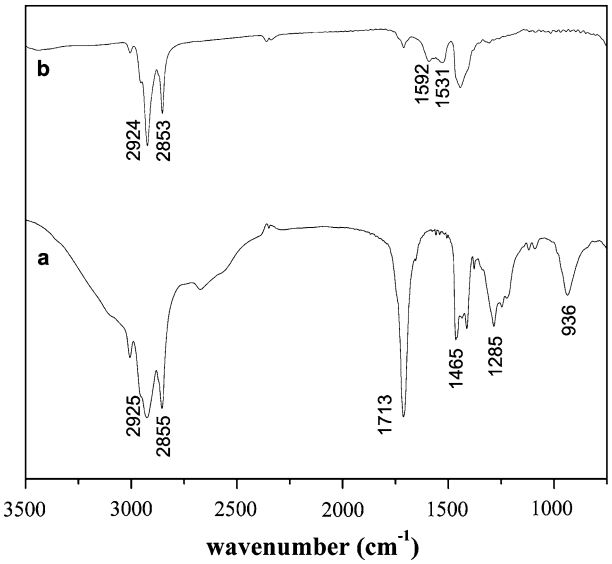

Fig. 2 FTIR spectra of **a** pure OA; **b** Fe_3O_4 coated with OA

the FTIR spectrum of OA-coated Fe_3O_4 (Fig. 2b), the asymmetric and symmetric CH_2 stretches were shifted to 2,924 and 2,853 cm^{-1}, respectively. The shifting to lower frequency indicates that the layer of surfactant molecules was adsorbed on to the solid surface and the hydrocarbon molecules surrounding the nanoparticles were in a closed-packed, crystalline state [17]. The C=O stretch, which was present at 1,713 cm^{-1} in Fig. 2a, was almost absent in the spectrum of OA-coated Fe_3O_4 (Fig. 2b). Two additional new bands appear at 1,592 and 1,531 cm^{-1}, characteristic of asymmetric and symmetric COO^- stretch. These results can be explained by the bonding of the carboxylic acids on the surface of the nanoparticles (Fig. 3) and hence these results confirm the formation of OA-coated Fe_3O_4.

PLGA nanoparticles

Size and morphology of the PLGA composite nanoparticles were determined by TEM. Figure 4 shows essentially spherical particles with an approximate diameter of around 200 nm. The black dots, i.e., the magnetite nanoparticles, appear to be spatially homogeneous within a single polymer nanosphere, at least approximately. There does seem to perhaps be some clustering of magnetite nanoparticles in a local sense within a sphere, but clustering is very difficult to discern from the 2-D image. Although the images printed here cannot be used directly to justify this statement, our examination of the images suggests that there is a more-or-less even distribution of magnetic nanoparticles between different composite particles.

The addition of magnetite increased the size of the PLGA particles slightly as shown in Table 1, but the size did not depend on the magnetite loading as long as some magnetite was present. The average hydrodynamic diameter of the particles

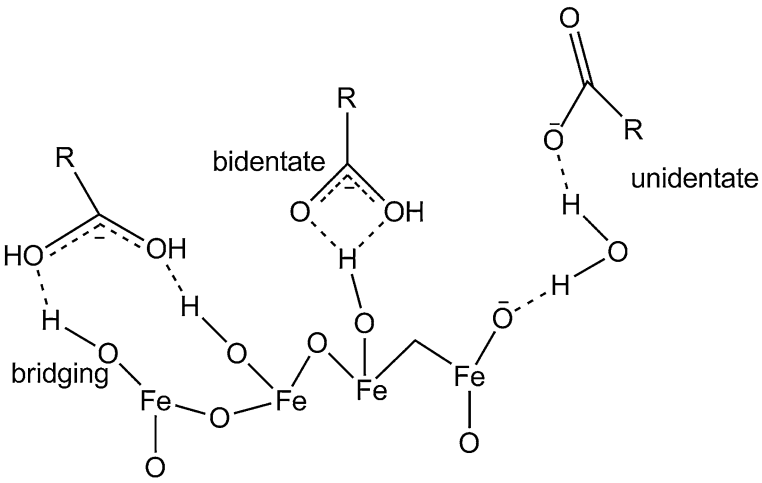

Fig. 3 Three possible interactions between OA and Fe_3O_4 [15]

measured by DLS was found to be 359 nm for PLGA nanoparticles, and an average of 387 nm for the particles with encapsulated magnetite, and was found to be 194 and 202 nm, respectively, as measured by TEM. The standard deviations reported in Table 1 are the variance of a single batch, not the variances in the means of different batches. Using TGA results described in the next paragraph, the volume fraction of magnetite in each PLGA particle is a factor of about three larger than the relative increase ($\sim$8 %) in diameter of each PLGA particle, i.e., each composite particle contains roughly the same absolute amount of PLGA as pure PLGA particles. The diameter obtained by DLS was about a factor of two larger than that determined via TEM, because PVA is expected to have a much smaller configuration when dried on TEM grid versus in water [6]. The zeta potential of composite nanoparticles measured was about -26 mV, and there are no significant difference in surface charge between the no-magnetite and magnetite-loaded PLGA particles (Table 1).

Figure 5 shows a representative TGA spectrum from a sample with encapsulated magnetite as well as that from magnetite after OA encapsulation. The increase in weight above 500 °C was assumed to be from magnetite oxidation and hence the minimum in the curve was used for determination of the weight fraction of magnetite. From the results, 56–62 % by weight of the composite particles consisted of magnetic nanoparticles (see Table 1). These encapsulation values of the hydrophobic magnetite were significantly higher than the maximum value in other studies, e.g., (13.5 % w/w at 1:1 ratio of magnetite:PLGA by double-emulsion method [15] and 40 % w/w in single oil-in-water emulsion) [19]. Moreover, the weight of PLGA was not an important factor in the incorporated magnetite inside the polymer, i.e., the weight of PLGA in solution changed by an order of magnitude, yet the fraction of magnetic particles in a composite particle changed by only 6 %. There are two possible explanations for this observation: either the fractional amount of PLGA that is transformed to a nanoparticle changes or the encapsulation efficiency of magnetite particles changes. Of course, both could be occurring. Other

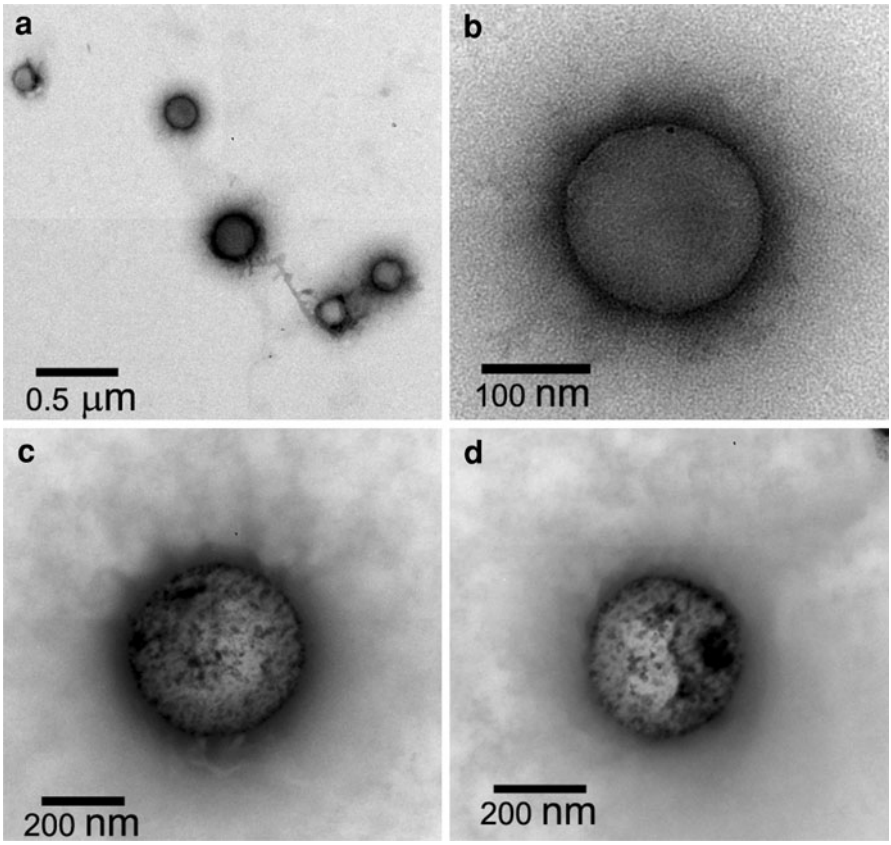

Fig. 4 TEM images of synthesized PLGA nanoparticles. **a** PLGA nanoparticles. **b** Pure PLGA. **c** 30 mg/ml PLGA (57 wt% magnetite). **d** 5 mg/ml PLGA (62 wt% magnetite)

Table 1 Size, surface charge, and magnetite loading of various weights of PLGA

Concentration of PLGA in oil phase (mg/ml)	Mean diameter measured by TEM (nm)	Mean diameter measured by DLS (nm)	Zeta potential (mV)	OA-Fe_3O_4 loading (wt%)
5 (no magnetite)	194 ± 21	358 ± 43	−26.8 ± 0.9	–
5	205 ± 30	379 ± 38	−25.5 ± 2.3	62.0
15	209 ± 26	380 ± 19	−24.6 ± 1.5	58.4
30	198 ± 25	400 ± 13	−25.9 ± 0.3	57.0
45	199 ± 24	382 ± 52	−25.5 ± 0.7	56.7
60	202 ± 22	394 ± 50	−24.1 ± 0.5	56.1

Unless otherwise indicated, magnetite concentration in the oil phase was 5 mg/ml

studies have changed the amount of encapsulated magnetite substantially [6, 15, 16, 20]. In all of these cases, the magnetite concentration inside the particles changed substantially; the magnetite content increased when increasing the weight

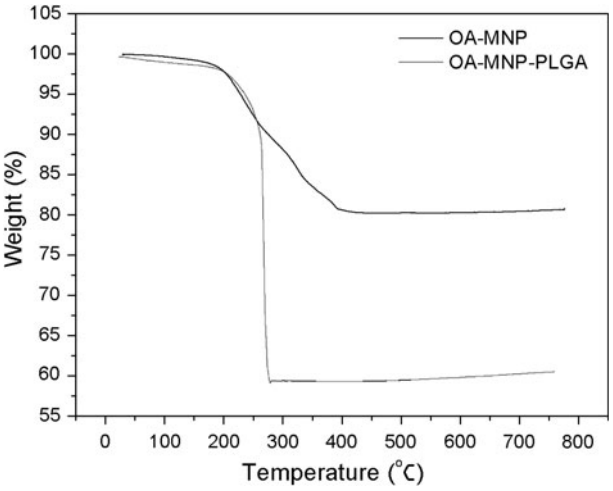

Fig. 5 Thermo-gravimetric curve of OA-coated magnetite and PLGA encapsulated magnetite

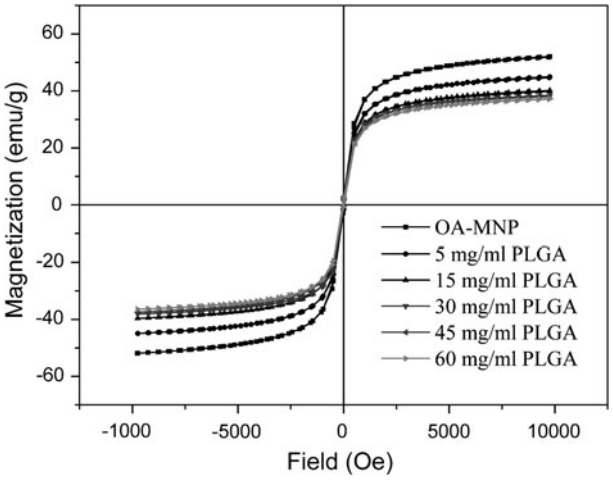

Fig. 6 Plot of magnetization of PLGA nanoparticles with magnetite incorporated inside

ratio of magnetite to polymer. Okassa et al. [20] did prepare sub-micron magnetite/PLGA particles by a modified double-emulsion method (w/o/w) with fixed amount of PLGA (100 mg) and magnetite amount in suspension was varied (50, 100, and 200 mg). When the volume of magnetite suspension increased the magnetite content increased, and an increase in the amount of polymer did not significantly affect the characteristics of nanocomposite particles except the magnetite content. In another case, Okassa et al. [15] prepared the composite sub-micron particles with a fixed amount of magnetite and varying PLGA concentration by simple emulsion/evaporation technique (w/o/w) at a magnetite/polymer ratio of 1:1, 1:1.5,

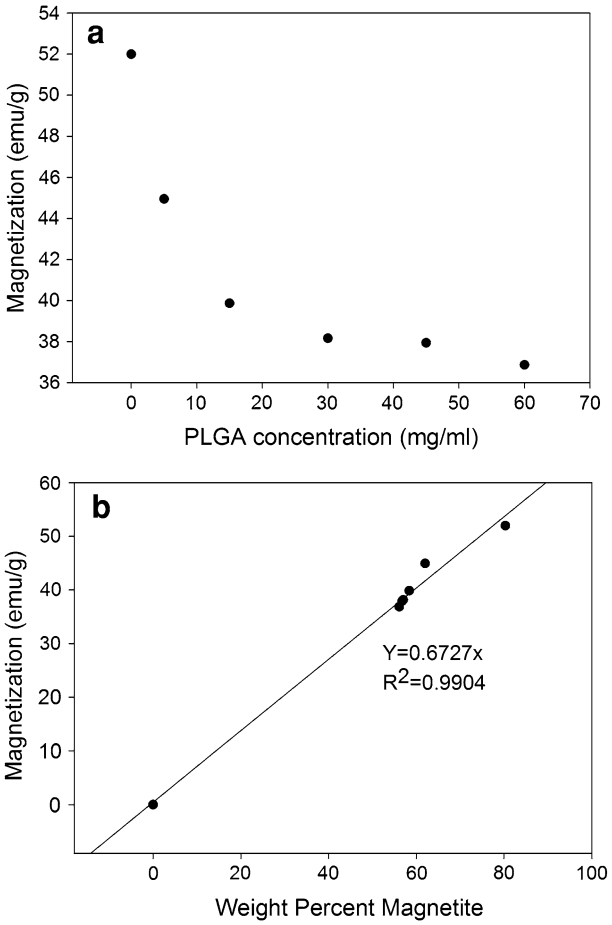

Fig. 7 **a** Magnetization of PLGA nanoparticles plotted versus OA-Fe_3O_4/PLGA weight ratio. **b** Magnetization of PLGA nanoparticles plotted versus weight percent of magnetite in PLGA particles

and 1:2 w/w. The magnetite loading increased with increasing the magnetite/polymer weight ratio.

Magnetization curves of the PLGA nanoparticles are shown in Fig. 6. These particles exhibited superparamagnetic behavior showing no hysteresis loop, indicating that these particles acted as a group of single-domain magnetic nanoparticles [20]. The highest saturation magnetization of the nanocomposites was 45 emu/g at 5 mg/ml PLGA and decreased with increasing PLGA concentration (Fig. 7a). The plot between the maximum magnetization of each concentration and the weight percent of magnetite in PLGA particles (Fig. 7b) indicates that over the very narrow range tested, the magnetization increases linearly with the content of magnetite inside the polymer. Note the 80 % point indicates pure Fe_3O_4; the value is not 100 % because this particle is surrounded by OA. The pure magnetite saturation magnetization was extrapolated to 67.3 emu/g. No magnetite oxidation, such as

that from the miniemulsion method described by Landfester and Ramirez [6], seems to have occurred as evidenced by the linear relationship as well as the fact that the extrapolated saturation magnetization at 100 % magnetite content compares favorably with other values such as 58 [21] and 50.3 emu/g [19].

Conclusion

Biodegradable PLGA nanoparticles containing superparamagnetic iron oxide nanoparticles were successfully synthesized by a double-emulsion method using OA-coated magnetite nanoparticles dispersed in the oil phase. Fe_3O_4 was equally distributed throughout the PLGA particles both in terms of in a given particle as well as across different particles. Increasing the amount of encapsulating PLGA polymer (5, 15, 30, 45, and 60 mg/ml of PLGA in the oil phase) at a constant 5 mg/ml of magnetite in the oil phase did not significantly affect the average hydrodynamic diameter of the particles although there was a slight increase versus PLGA with no encapsulated magnetite. Surprisingly, the encapsulated amount of magnetite was only very weakly dependent on the PLGA concentration. Saturation magnetizations were proportional to magnetite loading at these high magnetite loadings, which is very important since the higher the saturation magnetization, the lower the magnetic field required to achieve a given force on the particles.

Acknowledgments This study was funded by National Center of Excellent for Petroleum, Petrochemicals, and Advance Materials, Chulalongkorn University. BPG contributed to this study partly supported by the National Institutes of Health (Grant no. R21-00357540) and the Oklahoma Center for the Advancement of Science and Technology (Grant no. AR082-009).

References

1. Kluchova K, Zboril R, Tucek J, Pecova M, Zajoncova L, Safarik I, Mashlan M, Markova I, Jancik D, Sebela M, Bartonkova H, Bellesi V, Novak P, Petridis D (2009) Superparamagnetic maghemite nanoparticles from solid-state synthesis—their functionalization towards peroral MRI contrast agent and magnetic carrier for trypsin immobilization. Biomaterials 30(15):2855–2863. doi:10.1016/j.biomaterials.2009.02.023
2. Hong RY, Pan TT, Li HZ (2006) Microwave synthesis of magnetic Fe_3O_4 nanoparticles used as a precursor of nanocomposites and ferrofluids. J Magn Magn Mater 303(1):60–68. doi:10.1016/j.jmmm.2005.10.230
3. Chomoucka J, Drbohlavova J, Huska D, Adam V, Kizek R, Hubalek J (2010) Magnetic nanoparticles and targeted drug delivering. Pharm Res 62(2):144–149. doi:10.1016/j.phrs.2010.01.014
4. Lee SJ, Jeong JR, Shin SC, Kim JC, Chang YH, Chang YM, Kim JD (2004) Nanoparticles of magnetic ferric oxides encapsulated with poly(D,L latide-*co*-glycolide) and their applications to magnetic resonance imaging contrast agent. J Magn Magn Mater 272:2432–2433. doi:10.1016/j.jmmm.2003.12.416
5. Sun C, Lee JSH, Zhang MQ (2008) Magnetic nanoparticles in MR imaging and drug delivery. Adv Drug Del Rev 60(11):1252–1265. doi:10.1016/j.addr.2008.03.018
6. Wassel RA, Grady B, Kopke RD, Dormer KJ (2007) Dispersion of super paramagnetic iron oxide nanoparticles in poly(D,L-lactide-*co*-glycolide) microparticles. Colloid Surf A 292(2–3):125–130. doi:10.1016/j.colsurfa.2006.06.012

7. Gaihre B, Khil MS, Lee DR, Kim HY (2009) Gelatin-coated magnetic iron oxide nanoparticles as carrier system: drug loading and in vitro drug release study. Int J Pharm 365(1–2):180–189. doi:10.1016/j.ijpharm.2008.08.020
8. Hans ML, Lowman AM (2002) Biodegradable nanoparticles for drug delivery and targeting. Curr Opin Solid State Mater Sci 6(4):319–327
9. Cheng FY, Wang SPH, Su CH, Tsai TL, Wu PC, Shieh DB, Chen JH, Hsieh PCH, Yeh CS (2008) Stabilizer-free poly(lactide-*co*-glycolide) nanoparticles for multimodal biomedical probes. Biomaterials 29(13):2104–2112. doi:10.1016/j.biomaterials.2008.01.01
10. Arnold MM, Gonnan EM, Schieber LJ, Munson EJ, Berkland C (2007) NanoCipro encapsulation in monodisperse large porous PLGA microparticles. J Control Release 121(1–2):100–109. doi:10.1016/j.jconrel.2007.05.039
11. De Stefano D, De Rosa G, Maiuri MC, Ungaro F, Quaglia F, Iuvone T, Cinelli MP, La Rotonda MI, Carnuccio R (2009) Oligonucleotide decoy to NF-kappa B slowly released from PLGA microspheres reduces chronic inflammation in rat. Pharm Res 60(1):33–40. doi:10.1016/j.phrs.2009.03.012
12. Blanco-Prieto MJ, Lecaroz C, Renedo MJ, Kunkova J, Gamazo C (2002) In vitro evaluation of gentamicin released from microparticles. Int J Pharm 242(1–2):203–206
13. Corrigan OI, Li X (2009) Quantifying drug release from PLGA nanoparticulates. Eur J Pharm Sci 37(3–4):477–485. doi:10.1016/j.ejps.2009.04.004
14. Jain RA (2000) The manufacturing techniques of various drug loaded biodegradable poly(lactide-*co*-glycolide) (PLGA) devices. Biomaterials 21(23):2475–2490
15. Okassa LN, Marchais H, Douziech-Eyrolles L, Herve K, Cohen-Jonathan S, Munnier E, Souce M, Linassier C, Dubois P, Chourpa I (2007) Optimization of iron oxide nanoparticles encapsulation within poly(D,L-lactide-*co*-glycolide) sub-micron particles. Eur J Pharm Biopharm 67(1):31–38. doi:10.1016/j.ejpb.2006.12.020
16. Hamoudeh M, Al Faraj A, Canet-Soulas E, Bessueille F, Leonard D, Fessi H (2007) Elaboration of PLLA-based superparamagnetic nanoparticles: characterization, magnetic behaviour study and in vitro relaxivity evaluation. Int J Pharm 338(1–2):248–257. doi:10.1016/j.ijpharm.2007.01.023
17. Zhang L, He R, Gu HC (2006) Oleic acid coating on the monodisperse magnetite nanoparticles. Appl Surf Sci 253(5):2611–2617. doi:10.1016/j.apsusc.2006.05.023
18. Yang J, Park SB, Yoon HG, Huh YM, Haam S (2006) Preparation of poly epsilon-caprolactone nanoparticles containing magnetite for magnetic drug carrier. Int J Pharm 324(2):185–190. doi:10.1016/j.ijpharm.2006.06.029
19. Liu ZL, Liu YJ, Yao KL, Ding ZH, Tao J, Wang X (2002) Synthesis and magnetic properties of Fe_3O_4 nanoparticles. J Mater Synth Proc 10(2):83–87
20. Okassa LN, Marchais H, Douziech-Eyrolles L, Cohen-Jonathan S, Souce M, Dubois P, Chourpa I (2005) Development and characterization of sub-micron poly(D,L-lactide-*co*-glycolide) particles loaded with magnetite/maghemite nanoparticles. Int J Pharm 302(1–2):187–196. doi:10.1016/j.ijpharm.2005.06.024
21. Liu XQ, Kaminski MD, Guan YP, Chen HT, Liu HZ, Rosengart AJ (2006) Preparation and characterization of hydrophobic superparamagnetic magnetite gel. J Magn Magn Mater 306(2):248–253. doi:10.1016/j.jmmm.2006.03.049